CAE Analysis of Primary Shaft Systems in Great Five-Axis Turning-Milling Complex CNC Machine

Chih-Chiang Hong [*], Cheng-Long Chang, Nai-Rui Ou, Chien-Yu Lin

Department of Mechanical Engineering, Hsiuping University of Science and Technology, Taichung, Taiwan

Abstract

The design and analysis of primary shaft systems by using the commercial software of computer aided engineering (CAE) in the heavy industry field are novel. The research purpose is to provide the computational results for the construction of primary shaft systems in the five-axis turning-milling complex machine. The CAE with commercial software is used to analyze the linear static construction, stress and deformation for primary shaft systems in the great five-axis turning-milling complex computer numerical control (CNC) machine. It is desirable to compute and find the most external loads of primary shaft systems in the CNC machine which can be used to operate in safety condition and under its yield stress value of materials. The linear computational results of static stresses and displacements in primary shaft systems are obtained and investigated with the commercial SOLIDWORKS® 2014 simulation module.

1. Introduction

There are many researches for the primary shaft in the fields of the gear system, rotor system, pump regulator system, propulsion system and Hooke's joint system. In 2018, Chowdhury and Yedavalli [1] presented the study and investigation of natural frequencies in the coupled spinning gear shaft system. In 2018, Eftekhari et al. [2] presented the effects nonlinear electromagnetic forces on the steady state amplitude responses for a simply supported rotor system. In 2018, Zhang et al. [3] presented the numerical and experimental results of tilt angles in the high-speed shaft for electro-hydrostatic pump's regulator system. In 2017, Chowdhury and Yedavalli [4] presented the low speed study of coupled spur geared shaft system to investigate the natural frequencies and dynamic responses. In 2017, Huang et al. [5] presented the optimization study of marine propulsion shaft system to investigate the vibration transmission. In 2016, Zou et al. [6] presented the numerical results of natural frequencies and amplitude responses in the marine propulsion shafting system. In 2014, Bulut [7] presented the numerical results of finite element method (FEM) to investigate the dynamic stability of a shaft Hooke's joint system. In 2014, Han et al. [8] presented the numerical results of direct spectral method (DSM) to investigate the force responses of a slant cracked shaft in a geared rotor system. In 2013, Lahriri and Santos [9] presented the numerical and experimental results of contact forces of the shaft and the bearing in a rotor–stator system. In 2012, Adekunle et al. [10] presented the computer aided design (CAD) technique to study and design the shaft under various severest loadings. In 2012, Shahgholi and Khadem [11] presented the static results of multiple scales method to investigate the steady state response of the rotating shaft. In 2010, Lin and Chu [12] presented the investigation of frequency and transversal responses of the slant cracked shaft in a rotor system. In 2009, Hosseini and Khadem [13] presented the vibration results of perturbation method to investigate the time responses of the

* Corresponding author. E-mail address: cchong@mail.hust.edu.tw

Tel.: +886-919037599; Fax: +886-4-24961187

rotating shaft. In 1995, Bert and Kim [14] presented the studies and investigations of bending and buckling for the long, powerful driveshaft with laminated composite materials.

The author has some presentations on the application in commercial computer aided engineering (CAE) software for the turning-milling complex computer numerical control (CNC) machine. In 2018, Hong et al. [15] presented the CAE static analysis of secondary shaft systems of the great five-axis CNC machine by using SOLIDWORKS® module. Usually there are seven steps used in the processes of simulation with the software SOLIDWORKS® simulation module. In 2017, Hong et al. [16] presented the CAE dynamic structural analysis of the great five-axis CNC machine by using SOLIDWORKS® module. In 2016, Hong et al. [17] presented the CAE static structural analysis of the great five-axis CNC machine by using SOLIDWORKS® module. The purpose of the research is to provide some computational results to design the primary shaft system in the five-axis turning-milling complex CNC machine. The linear static results of stresses and displacements of the primary shaft systems are obtained and investigated with the SOLIDWORKS® 2014 simulation module. The maximum values of stress and displacement are obtained to give a safety prediction for the design of primary shaft systems due to external axial pressure loads and torsion loads. The novelties are to present the designs of primary shaft systems in CNC machines by using the commercial CAE for engineers and to investigate the simulation data for the primary shaft systems under external pressure and torsion loads.

2. Method of simulations

2.1. Mathematical model and software

In the linear static structural analysis, a general mathematical model in matrix form would be given and used in the computer program to solve for stress and displacement results. Generally, there are some steps used in the method of simulation with the software SOLIDWORKS® simulation module to find the results of displacement and stress [15]. Assumptions involved in the study are for the inner part in gear trains by using the simplify shapes, for the geometry of the cut tool by using the upper right end shaft to simulate the milling.

2.2. Assembling 3D parts
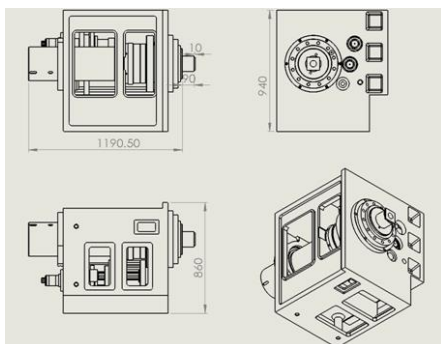
(a) Dimensions of primary shaft systems   (b) Assembling 3D parts of primary shaft systems
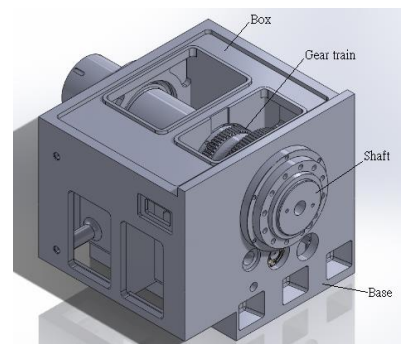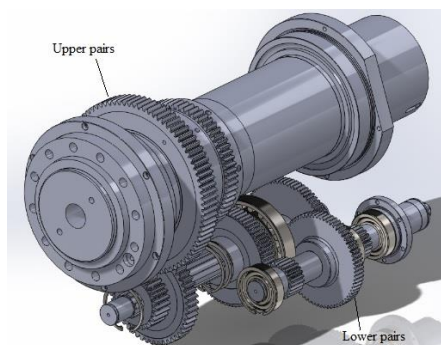
(c) Shafts in primary shaft systems   (d) Upper pairs gear train in primary shaft systems

Fig. 1 Dimensions and assembling 3D parts of primary shaft systems

To use the commercial CAE software and run the static results for complex CNC machine, it is necessary to prepare the assembling 3D parts of primary shaft systems as shown in Fig. 1. The dimensions of the main parts are provided for primary shaft system with 1190.5 mm, 940 mm and 860 mm as shown in Fig. 1(a). The main components of the primary shaft system are geared trains, shafts and box as shown in Figs. 1(b)-1(d). The dimensions of interior parts of the gearbox like shaft and gears are upper shaft diameter is 209 mm, upper right end shaft diameter is 110 mm, upper big gear diameter is 440 mm, lower shaft diameter is 20 mm, lower small gear diameter is 40 mm, lower big gear diameter is 120 mm, respectively. There are upper pairs and lower pairs, gear trains composed the gear train system to transmit the rotation speed for the shafts as shown in the Fig. 1(c). The tool is fixed on the end of gear shaft to provide drilling and milling functions. The primary shaft system can be rotated by the base in rotational motion with respect to Y axis.

2.3. Materials of 3D parts

It is necessary to define the individual material of assembling 3D parts for great five-axis turning-milling complex CNC machine. The materials of the main parts of the primary shaft systems are given with cast iron and steel alloy. The yield stress of cast iron material for the primary shaft system is 275MPa. The yield stress of the steel alloy material for the gear train system is 620MPa. To prevent failure in the CNC machine, the value of working stress in each material of components should be under its yield stress value.

2.4. Boundary conditions of primary shaft systems

The boundary conditions of primary shaft systems are used to compute and analyzed corresponding to external loads locate at position with 100 mm apart along the X axis of the head of gear shaft. Boundary conditions of primary shaft systems are shown in Fig. 2. Clamp boundary conditions of the base in the box of the primary shaft system are shown in Fig. 2(a). External loads (torsion) locate at position typically on the right end of the primary shaft system is also shown in Fig. 2(a). When the detail structural design of the gear train study is needed, the boundary conditions of upper pairs, gear train in the primary shaft system is shown in Fig. 2(b). The clamp boundary conditions of box, shaft and gear train are specified in green color arrows in Fig. 2 of the works, respectively. External loads (axial pressure) are typically located on the right end of the gear is also shown in Fig. 2(b).

(a) Boundary conditions in the base of box   (b) Boundary conditions in upper pairs gear train
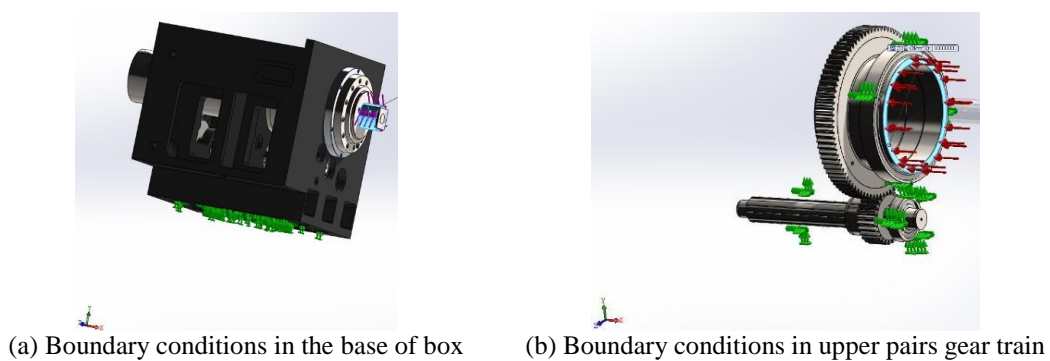
Fig. 2 Boundary conditions of primary shaft systems

2.5. Properly parameter of meshes

It is critical to gain a mesh convergence and a good element before the CAE simulation. For the convenience, grid-mesh with proper mesh controlled based on the size of parts, medium mesh density, and used to generate a proper grid-mesh. When the values of the results, e.g. maximum displacement changed less than or equal to 1e-06, thus the mesh would be in the good convergence condition, and this mesh of elements can be used for the further analysis of the CAE simulations. A typical grid-mesh for the primary shaft systems is shown in Fig. 3. With proper parameter element length based on standard mesh is used to generate a proper grid-mesh in the computation and analyses. Grid-mesh in primary shaft system for gear shaft is shown in Fig. 3(a). Grid-mesh in the upper pairs and lower pairs, gear trains system are shown in Figs. 3(b) and 3(c), respectively.
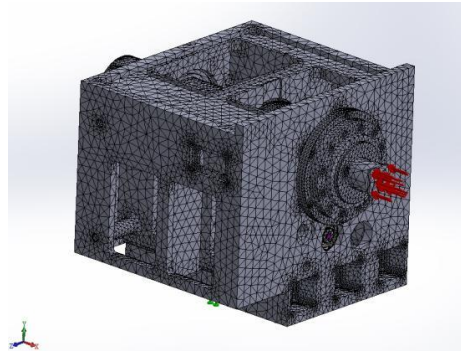
(a) Grid-mesh in primary shaft systems
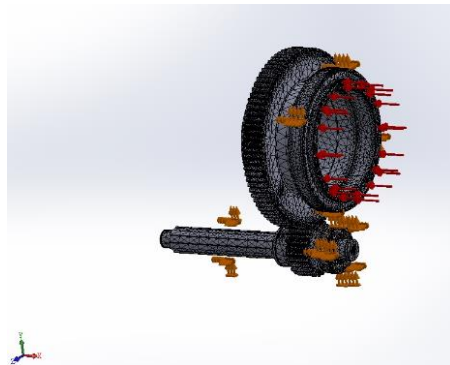
(b) Grid-mesh in the upper pairs gear train   (c) Grid-mesh in the lower pairs gear train
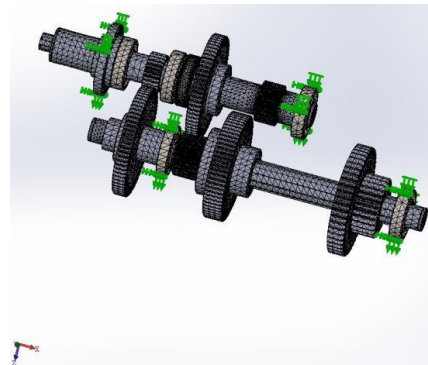
Fig. 3 Typical grid-mesh for the primary shaft systems

3. Results and Discussion

3.1. Static results due to external loads
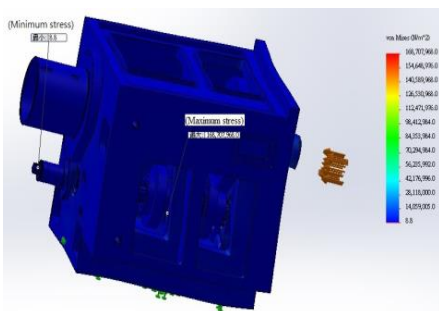
(a) Stress for the shaft system due to axial 10MPa is parallel to X axis
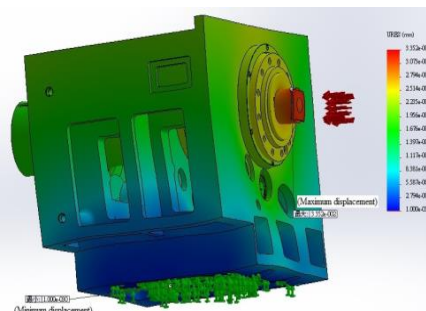
(b) Displacement for the shaft system due to axial 10MPa is parallel to X axis
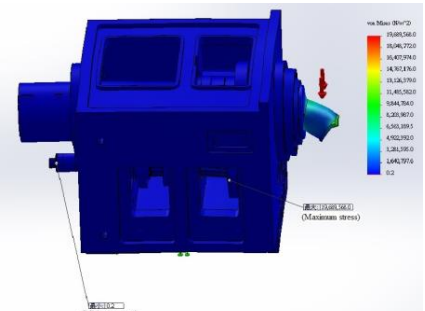
(c) Stress for the shaft system due to axial 10MPa is parallel to Y axis
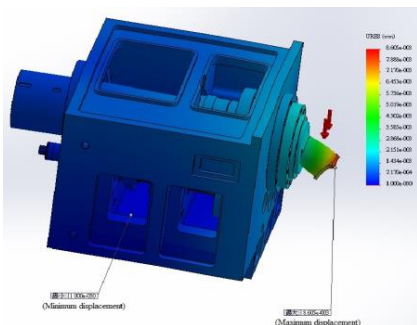
(d) Displacement for the shaft system due to axial 10MPa is parallel to Y axis
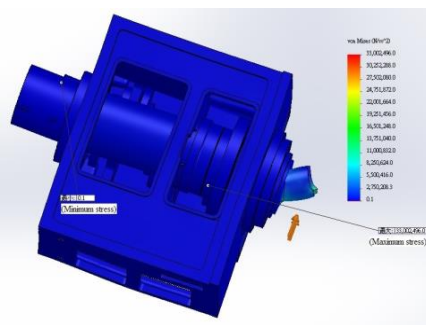
(e) Stress for the shaft system due to axial 10MPa is parallel to Z axis
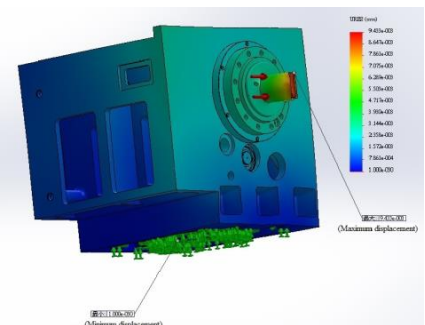
(f) Displacement for the shaft system due to axial 10MPa is parallel to Z axis

Fig. 4 Stress and displacement for the shaft system due to axial 10MPa external loads

Firstly, use the SOLIDWORKS® 2014 simulation module to obtain the stresses and displacements of static results due to external axial pressure loads (10MPa) on the right end head of primary shaft systems. Static stress and displacement results of the primary shaft due to axial pressure value 10MPa is perpendicular to Y-Z plane and parallel to X axis are shown in Figs. 4(a) and 4(b), respectively. The maximum value 168MPa of stresses is found in the left pitch area of lower pairs, gear train and the maximum value 0.03352 mm of displacements is found in the top area of shaft head. Static stress and displacement results of the primary shaft due to axial pressure value 10MPa is perpendicular to X-Z plane and parallel to Y axis are shown in Figs. 4(c) and 4(d), respectively. The maximum value 19MPa of stresses is found in the right pitch area of lower pairs, gear train and the maximum value 0.008606 mm of displacements is found in the top area of shaft head. Static stress and displacement results of the primary shaft due to axial pressure value 10MPa is perpendicular to X-Y plane and parallel to Z axis are shown in Figs. 4(e) and 4(f), respectively. The maximum value 33MPa of stresses is found in the right pitch area of upper pairs gear train and the maximum value 0.009433 mm of displacements is found in the top area of shaft head.

Table 1 Maximum stresses and displacements for the primary shaft

External loads	Maximum stress	Maximum displacement
When axial 10MPa is parallel to X axis	168MPa	0.03352mm
When axial 10MPa is parallel to Y axis	19MPa	0.008606mm
When axial 10MPa is parallel to Z axis	33MPa	0.009433mm
When torsion 10000Nm is parallel to X axis	72MPa	0.02728mm

Secondly, to obtain the static results of stresses and displacements due to external torsion loads (10000Nm) on the right end head of primary shaft systems. Static stress and displacement results of primary shaft systems due to torsion value 10000Nm is parallel to X axis are shown in Figs. 5(a) and 5(b), respectively. The maximum value 72MPa of stresses is found in the area of shaft head and the maximum value 0.02728 mm of displacements is found in the top area of shaft head. Maximum stresses and displacements for the primary shaft due to external loads are listed in the Table 1. The maximum stresses are found in the values smaller than the yield stress value 275MPa of cast iron material for the primary shaft system. It is suggested that the primary shaft can stand greater and over than external loads with pressure value 10MPa and torsion value 10000Nm. It is also necessary to find the more detailed data for the design of lower pairs gear train systems, since the dominated, maximum value 168MPa of stresses is found in the left pitch area of the lower pairs gear train due to pressure value 10MPa and torsion value 10000Nm. Factor of safety in the design value is more than or equal to 1, it can also be considered as the static work by using the ratio value of maximum stress vs. external load. E.g. for the maximum stress value is 168MPa in the Table 1: if the factor of safety value 1.5 has been used, then the value of allowed external load is 168MPa/ 1.5 and that is where 112MPa can be loaded; if the higher value of the factor of safety 2.0 has been used, then the smaller value of allowed external load is 168MPa/ 2.0 and that is where 84MPa can be loaded on the gear train systems.

(a) Stress for the shaft system due to torsion (10000Nm) is parallel to X axis

(b) Displacement for the shaft system due to torsion (10000Nm) is parallel to X axis
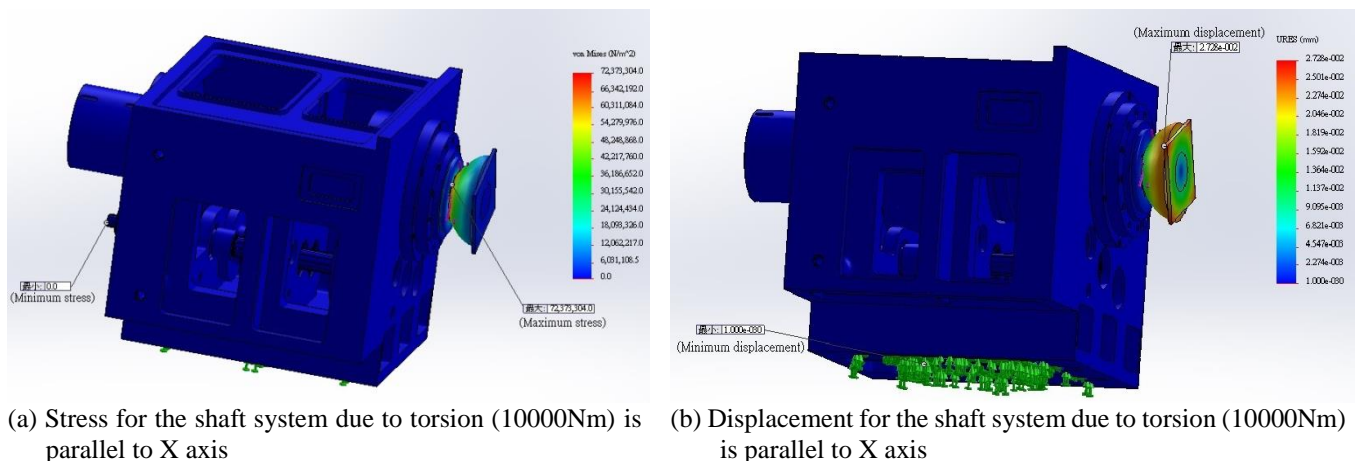
Fig. 5 Stress and displacement for the shaft system due to torsion (10000Nm) is parallel to X axis

3.2. Static results for the gear train systems
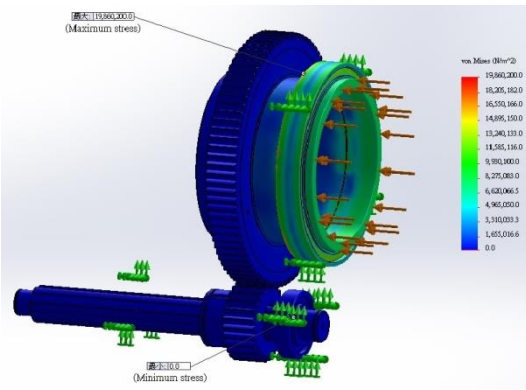
(a) Stress for the upper pairs gear train due to axial 10MPa is parallel to X axis
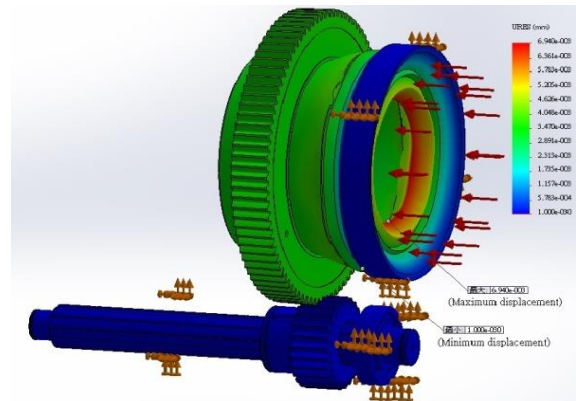
(b) Displacement for the upper pairs gear train due to axial 10MPa is parallel to X axis
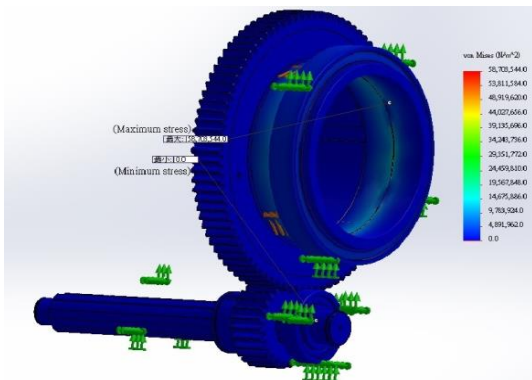
(c) Stress for the upper pairs gear train due to torsion (10000Nm) is parallel to X axis
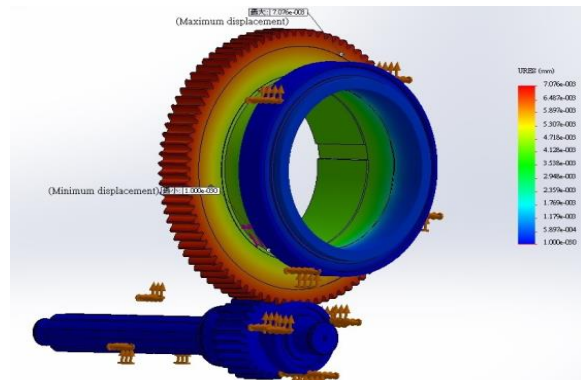
(d) Displacement for the upper pairs gear train due to torsion (10000Nm) is parallel to X axis
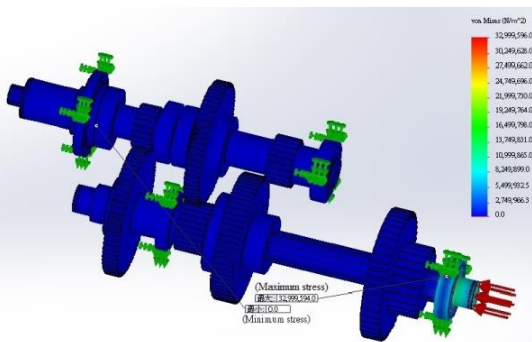
(e) Stress for the lower pairs gear train due to axial 10MPa is parallel to X axis
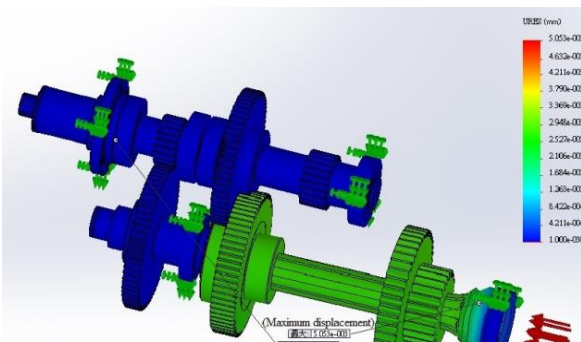
(f) displacement for the lower pairs gear train due to axial 10MPa is parallel to X axis
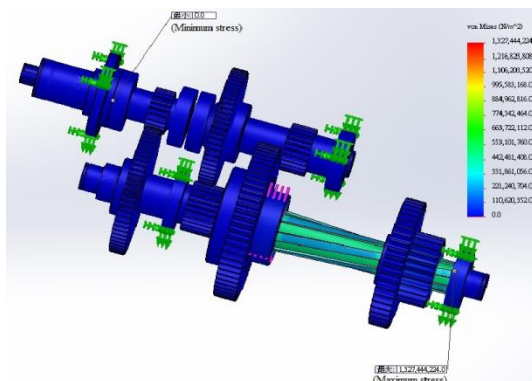
(g) Stress for the lower pairs gear train due to torsion (10000Nm) is parallel to X axis
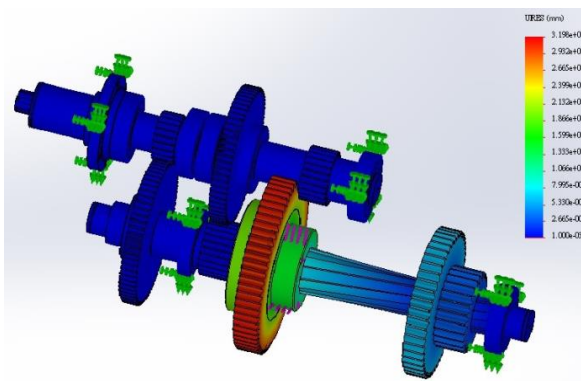
(h) displacement for the lower pairs gear train due to torsion (10000Nm) is parallel to X axis

Fig. 6 Stress and displacement for the upper and lower pairs gear train due to external loads

For the precision and more detailed design of lower pairs gear train systems, it can also be used in SOLIDWORKS® 2014 simulation module to obtain the stresses and displacements of static results due to external axial pressure loads (10MPa) and torsion loads (10000Nm) on the gear train systems. Static stress and displacement results of upper pairs gear train due to axial pressure value 10MPa is parallel to X axis are shown in Figs. 6(a) and 6(b), respectively. The maximum value 19.8MPa of stresses are found in the upper bearing area of upper pairs gear train and the maximum value 0.00694 mm of displacements is found in the inner position of the upper bearing area of upper pairs gear train. Static stress and displacement results of upper pairs gear train due to axial torsion value 10000Nm is parallel to X axis are shown in Figs. 6(c) and 6(d), respectively. The maximum value 58.7MPa of stresses are found in the inner position of the upper bearing area of upper pairs gear train and the maximum value 0.007076 mm of displacements is found in the upper area of upper pairs gear train. Static stress and displacement results of lower pairs gear train due to axial pressure value 10MPa is parallel to X axis are shown in Figs. 6(e) and 6(f), respectively. The maximum value 32.9MPa of stresses is found in the upper bearing area of lower pairs gear train and the maximum value 0.005053 mm of displacements is found in the outer position of the upper bearing area of lower pairs gear train. Static stress and displacement results of lower pairs gear train due to axial torsion value 10000Nm is parallel to X axis are shown in Figs. 6(g) and 6(h), respectively. The maximum value 1327MPa of stresses is found in the upper bearing area of lower pairs gear train and the maximum value 3.198 mm of displacements is found in the outer position of the upper gear area of the lower pairs gear train. The maximum stress value 1327MPa is found in the value greater than the yield stress value 620MPa of steel alloy material for the gear train systems. It is suggested that the gear train system cannot stand greater and over than external loads with torsion value 10000Nm. In the linear value of calculation under the torsion value 4672Nm for the gear train system of the CNC machine can be considered in safety condition.

4. Conclusions

The static results of stresses and displacements of a primary shaft system of CNC machines are obtained with the SOLIDWORKS® 2014 simulation module. The static maximum stress and displacement for the types of clamp boundary conditions of primary shaft and gear trains are studied. It is desired to compute and find the most of the external load of primary shaft systems in the CNC machine, which can be used to operate in safety condition under its yield stress value of materials. The maximum values of stress due to the effect of typical external loads e.g. axial pressure and axial torsion are all smaller than yield stress value, so the CNC machine can be considered in safety condition. The combined effect of axial and torsion loads can be considered in the linear work by summing the corresponding results of divisional load. Factor of safety in the design value is more than or equal to 1 can also be considered in the static work by using the ratio value of maximum stress vs. external load. To provide some highlight results in detailed as follows, (1) it is helpful for engineers to investigate great five-axis turning-milling complex CNC machine data under CAE analysis, (2) commercial CAE solution for the primary shaft systems under external pressure and torsion loads is provided, (3) the linear results are provided by using the simulation module of SOLIDWORKS® .

Conflicts of Interest

The authors declare no conflict of interest.

References

[1] S. Chowdhury and R. K. Yedavalli, "Vibration of high speed helical geared shaft systems mounted on rigid bearings," International Journal of Mechanical Sciences, vol. 142-143, pp. 176-190, 2018.
[2] M. Eftekhari, A. D. Rahmatabadi, and A. Mazidi, "Nonlinear vibration of in-extensional rotating shaft under electromagnetic load," Mechanism and Machine Theory, vol. 121, pp. 42-58, 2018.
[3] J. Zhang, Y. Chen, B. Xu, M. Pan, and Q. Chao, "Effects of splined shaft bending rigidity on cylinder tilt behaviour for high-speed electro-hydrostatic actuator pumps," Chinese Journal of Aeronautics, in press.

[4]   S. Chowdhury and R. K. Yedavalli, "Dynamics of low speed geared shaft systems mounted on rigid bearings," Mechanism and Machine Theory, vol. 112, pp. 123-144, 2017.

[5]   X. Huang, Z. Ni, Z. Zhang, and H. Hua, "Stiffness optimization of marine propulsion shafting system by FRF-based substructuring method and sensitivity analysis," Ocean Engineering, vol. 144, pp. 243-256, 2017.

[6]   D. Zou, L. Liu, Z. Rao, and N. Ta, "Coupled longitudinal–transverse dynamics of a marine propulsion shafting under primary and internal resonances," Journal of Sound and Vibration, vol. 372, pp. 299-316, 2016.

[7]   G. Bulut, "Dynamic stability analysis of torsional vibrations of a shaft system connected by a Hooke's joint through a continuous system model," Journal of Sound and Vibration, vol. 333, pp. 3691-3701, 2014.

[8]   Q. Han, J. Zhao, W. Lu, Z. Peng, and F. Chu, "Steady-state response of a geared rotor system with slant cracked shaft and time-varying mesh stiffness," Communications in Nonlinear Science and Numerical Simulation, vol.19, pp. 1156-1174, 2014.

[9]   S. Lahriri and I. F. Santos, "Theoretical modelling, analysis and validation of the shaft motion and dynamic forces during rotor–stator contact," Journal of Sound and Vibration, vol. 332, pp. 6359-6376, 2013.

[10] A. A. Adekunle, S. B. Adejuyigbe, and O. T. Arulogun, "Development of CAD software for shaft under various loading conditions," Procedia Engineering 38, 2012, pp. 1962-1983.

[11] M. Shahgholi and S. E. Khadem, "Primary and parametric resonances of asymmetrical rotating shafts with stretching nonlinearity," Mechanism and Machine Theory, vol. 51, pp. 131-144, 2012.

[12] Y. Lin and F. Chu, "The dynamic behavior of a rotor system with a slant crack on the shaft," Mechanical Systems and Signal Processing, vol. 24, pp. 522-545, 2010.

[13] S. A. A. Hosseini and S. E. Khadem, "Combination resonances in a rotating shaft," Mechanism and Machine Theory, vol. 44, pp. 1535-1547, 2009.

[14] C. W. Bert and C. D. Kim, "Analysis of buckling of hollow laminated composite drive shafts," Composites Science and Technology, vol. 53, pp. 343-351, 1995.

[15] C. C. Hong, C. L. Chang, C. C. Huang, C. C. Yang, and C. Y. Lin, "CAE analysis of secondary shaft systems in great five-axis turning-milling complex CNC machine," Advance in Technology Innovation, vol. 3, pp. 43-50, 2018.

[16] C. C. Hong, C. L. Chang, and C. Y. Lin, "Dynamic structural analysis of great five-axis turning-milling complex CNC machine," Global Journal of Researches in Engineering: A, Mechanical and Mechanics Engineering, vol. 17, pp. 1-8, 2017.

[17] C. C. Hong, C. L. Chang, and C. Y. Lin, "Static structural analysis of great five-axis turning-milling complex CNC machine," Engineering Science and Technology, an International Journal, vol. 19, pp. 1971-1984, 2016.